Determination of reaction geometries

Karl-Heinz Gericke

Institut für Physikalische und Theorestische Chemie, Technische Universität Braunschweig, Hans-Sommer-Strasse 10, D-38106 Braunschweig, Germany

Christoph Kreher

Institut für Physikalische Chemie, Universität Zürich, Winterthurerstr. 190, CH-8057 Zürich

Ernst Albrecht Reinsch

Institut für Physikalische und Theoretische Chemie, Universität Frankfurt, Marie-Curie-Strasse 11, D-60439 Frankfurt a. M., Germany

Using polarized light the reaction geometry of selected species can be controlled even in bulk experiments. One reactant A is generated in a photodissociation process and its spatial distribution is completely described by the anisotropy parameter β. The other molecular reactant B is excited in a specific rovibrational state. Its spatial distribution is given by the J- and branch-dependent alignment parameter $A_0^{(2)}$. Equations have been developed that allow a relatively easy conversion of experimental results to the angle of attack, γ. The unnormalized probability of an attack of A on B under an angle γ is given by the simple expression $P(\gamma) \propto [1 + \frac{1}{5}\beta A_0^{(2)} P_2(\cos \gamma) P_2(\cos \delta)]$ where δ is the angle between the $\vec{E}$ vectors of the dissociating and the exciting laser beam. As an example, we have studied the reaction of $A + HCN \rightarrow HA + CN$ with A=H,Cl. The experimental results prove a preferred linear reaction geometry, i.e, an end-on attack of atom A on the terminating hydrogen atom of the HCN reactant. However, the cone of acceptance is higher for the Cl+HCN reaction than for the H+HCN one. © *1997 American Institute of Physics.* [S0021-9606(97)01947-8]

I. INTRODUCTION

In general, chemical reactions are influenced by steric effects. In organic chemistry special groups are used to protect the molecule from an unwanted spatial attack of a reactant. In order to control the reaction geometry of small systems different techniques have been used, like the electric field orientation[1,2] and the brute force method,[3,4] also known as orientation of molecules in pendular states.[5] If there is any preferred angle of attack, $\gamma(A,B)$, a variation of the reactant approach geometry will influence the reaction rates. In this work polarized light is used to induce anisotropic reactants distributions of the species A and B in the lab frame. We want to develop a quantitative description of extracting the average attack angle γ from experimental observations, when linearly polarized light is used to align the reactants. Although only two specific reactions of the HCN molecule are experimentally analyzed as an example, such experiments, in general, allow a detailed insight into the stereodynamics of the bimolecular reaction under investigation.

A schematic representation of the alignment of reactants is shown in Fig. 1.

One reactant, A, is generated in the photodissociation of a precursor molecule, X–A. The direction of the recoil velocity $\vec{v}$ is determined by the anisotropy parameter β. The ϑ dependence with respect to the $\vec{E}_v$ vector of the *dissociating* laser light is given by the simple expression[6]

$$\rho_v(\vartheta, \phi) = \frac{1}{4\pi} [1 + \beta P_2(\cos \vartheta)], \qquad (1a)$$

where $P_2(\cos \vartheta) = (3 \cos^2 \vartheta - 1)/2$ is Legendre's polynomial of order 2. Under these experimental conditions the dissocia-

tion geometry is of cylindrical symmetry, indicated by the absence of a φ dependence. The β parameter ranges from $+2$ for a pure $\cos^2 \vartheta$ distribution to -1 for a pure $\sin^2 \vartheta$ distribution; $\beta = 0$ describes a complete isotropic direction of recoil. Usually precursor molecules can be found that fragment near the extreme values of β, guaranteeing a distinct distribution of the reactant A in the lab frame.

The partner reactant B will be prepared by excitation of a rovibrational state of the electronic ground state. In general, the corresponding transition dipole moment of a linear molecular reactant B lies along the internuclear axis and, therefore, the linearly polarized laser beam selects molecules according to a $\cos^2 \theta$ distribution, where θ is measured from the $\vec{E}_J$ vector of the *exciting* laser beam. Thus, the initial cylindrical symmetry is broken.

Zare and co-workers[7] showed that the spatial distribution of an excited molecule using polarized light, $\vec{E}_J$, depends on the branch of excitation. The J-dependent spatial distribution,

$$\rho_J(\theta, \phi) = \frac{1}{4\pi} [1 + A_0^{(2)} P_2(\cos \theta)], \qquad (1b)$$

is described by the alignment parameter $A_0^{(2)}$ (cf. Fig. 2):

$$A_0^{(2)} = \begin{cases} \dfrac{J-1}{2J+1}, & P \text{ branch,} \\[2ex] \dfrac{J+2}{2J+1}, & R \text{ branch.} \end{cases} \qquad (2)$$

The highest alignment can be achieved for the lowest R-branch excitation [$R(0):A_0^{(2)}=2$]. On the other hand, the
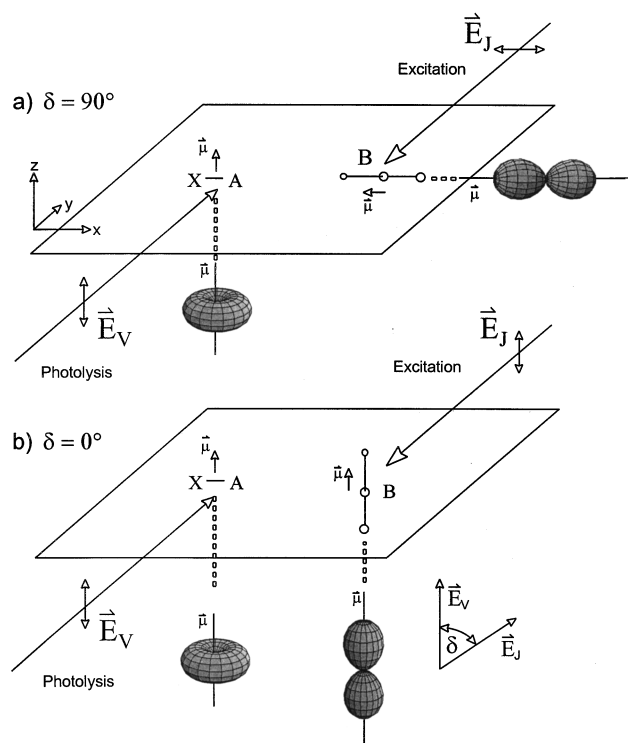
FIG. 1. Pictorial view of controlling the reaction geometry by the use of polarized light.

lowest P transition, $P(1)$, leads to no alignment of the reactant because the upper excited state is $J=0$, which has spherical symmetry. It is very important to remember that this spatial distribution of reactant B is measured by θ (with respect to $\vec{E}_J$), while the recoil direction of reactant A is characterized by ϑ, which is measured with respect to $\vec{E}_v$. The motivation of the present paper is a ''conjunction'' of these two distributions that will allow a quantitative description of the reaction geometry.
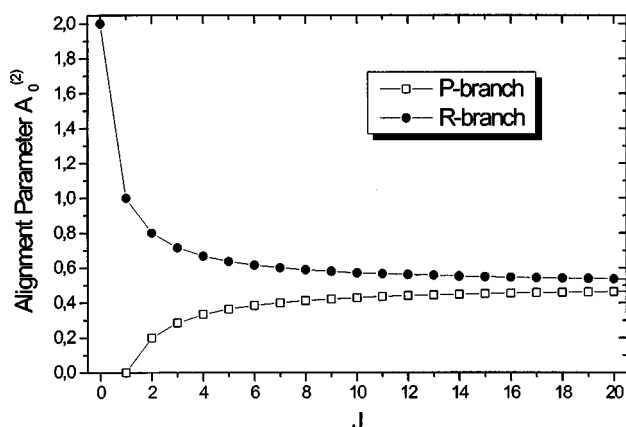

FIG. 2. J dependence of the rotational alignment parameter $A_0^{(2)}$ for the P and R branches.

II. THEORY

The spatial distribution of the reactant A, i.e., the ϑ and φ dependence with respect to $\vec{E}_J$, is given by the simple expression (1a). In the following it is useful to describe this distribution by spherical harmonics:[8]

$$\rho_V(\vartheta,\varphi) = \frac{1}{\sqrt{4\pi}} \left(Y_{00}(\vartheta,\varphi) + \frac{\beta}{\sqrt{5}} Y_{20}(\vartheta,\varphi) \right), \quad (3)$$

where the z axis ($\vartheta=0$) is in the direction of the field strength of the dissociation laser, $\vec{E}_v$.

The spatial distribution of the excited reactant B, $\rho_J(\theta,\phi)$, depends on the state and branch that is used for excitation. If we assume no special rotational vibrational interaction then the rotational contribution for P-branch ($J \to J-1$) and R-branch ($J \to J+1$) excitation is given by[7]

$$\rho_J^{(P)}(\theta,\phi) = \frac{J}{3\sqrt{4\pi}} \left(Y_{00}(\theta,\phi) + \frac{1}{\sqrt{5}} \frac{J-1}{2J+1} Y_{20}(\theta,\phi) \right), \quad (4a)$$

$$\rho_J^{(R)}(\theta,\phi) = \frac{J+1}{3\sqrt{4\pi}} \left(Y_{00}(\theta,\phi) + \frac{1}{\sqrt{5}} \frac{J+2}{2J+1} Y_{20}(\theta,\phi) \right), \quad (4b)$$

where we describe again the distributions by spherical harmonics. Here, the z axis ($\theta=0$) is the direction of $\vec{E}_J$.

In order to obtain the probability that the atom A hits the molecule B under the angle γ (Fig. 1) one has to sum up all angular variables $(\Omega;\Omega') = (\theta,\phi,\vartheta,\varphi)$, which lead to the angle γ between the two directions:

$$P(\gamma) = \int_\Omega \int_{\Omega'} [\rho_J(\theta,\phi)\rho_v(\vartheta,\varphi)]_\gamma \, d\Omega' \, d\Omega. \quad (5)$$

Taking into account this constraint, the above integral is a three fold one and its calculation is given in the Appendix. The result is

$$P^P(\gamma,\delta) = \frac{J\sin\gamma}{6}$$
$$\times \left(1 + \frac{\beta}{5} \frac{J-1}{2J+1} P_2(\cos\gamma)P_2(\cos\delta) \right], \quad (6a)$$

$$P^R(\gamma,\delta) = \frac{(J+1)\sin\gamma}{6}$$
$$\times \left[1 + \frac{\beta}{5} \frac{J+2}{2J+1} P_2(\cos\gamma)P_2(\cos\delta) \right]. \quad (6b)$$

δ is the angle between the two laser polarization directions $\vec{E}_J$ and $\vec{E}_v$. The J dependence of $P(\gamma,\delta)$ in the square brackets is the rotational alignment described by the branch-dependent quantity $A_0^{(2)}$. Thus, the (unnormalized) probability of $P(\gamma,\delta)$ is given by

$$P(\gamma,\delta) \propto [1 + \tfrac{1}{5}\beta A_0^{(2)} P_2(\cos\gamma)P_2(\cos\delta)]. \quad (7)$$

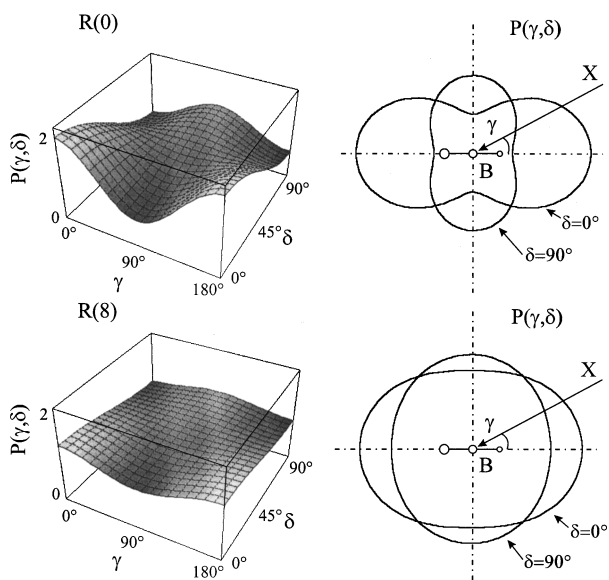FIG. 3. Unnormalized plot of $P(\gamma,\delta)$ describing the probability that an atom A, which is generated in a photodissociation process characterized by $\beta=2$, attacks a molecule at angle γ, where the molecule is prepared by a $R(0)$ or $R(8)$ transition. δ is the angle between the two $\vec{E}$ vectors of the photolysis and of the exciting laser beam. The important experimental situation of $\delta=0°$ and $\delta=90°$ is shown in a polar plot.

FIG. 4. Plot of $P(\gamma,\delta)$ for the case that the spatial recoil direction is described by $\beta=-1$.

It should be mentioned that Simpson et al.[9] derived an expression of similar form under the assumption of cylindrical symmetry that is justified for their experiments on steric effects in the reaction of Cl with CH_4 and CHD_3.

In order to gain insight into the intensity differences that might occur when the reaction proceeds under different angles of attack γ, it is useful to compare Eq. (7) for the case of $\delta=0°$ and $R(0)$ excitation,

$$P(\gamma,0°)^{R(0)} \propto [1 + \tfrac{2}{5}\beta P_2(\cos \gamma)], \qquad (8)$$

with the well-known equation for photodissociation processes [Eq. (1)].

Equation (8) is almost equivalent to Eq. (1a), with the exception that the anisotropy factor β is reduced to 40%. The reduction in signal differences when going from dissociation to reactive processes is not very surprising because averaging reduces the initial spatial alignment of the reactants.

A two-dimensional plot of $P(\gamma,\delta)$ for $R(0)$ and $R(8)$ excitation is shown in Fig. 3. The β parameter is $\beta=2$, i.e. a parallel transition of the precursor molecule is used. Such photodissociation processes should be preferred when the stereodynamics of a reaction is studied because the highest selectivity can be achieved. The reason for this higher selectivity is a substantial reduction in the likelihood of a side-on attack for $\vec{E}_v\|\vec{E}_J$. As one expects, the largest difference in intensities can be observed between $\delta=0°$ and $\delta=90°$. Thus, a change of the alignment of the two $\vec{E}$ vectors of the photolysing laser beam, $\vec{E}_v$, and of the exciting beam, $\vec{E}_J$, will induce the largest difference in the product generation, if there is any stereodynamic effect in the reaction under study. Therefore, $P(\gamma)$ is plotted in a polar diagram (Fig. 3) for
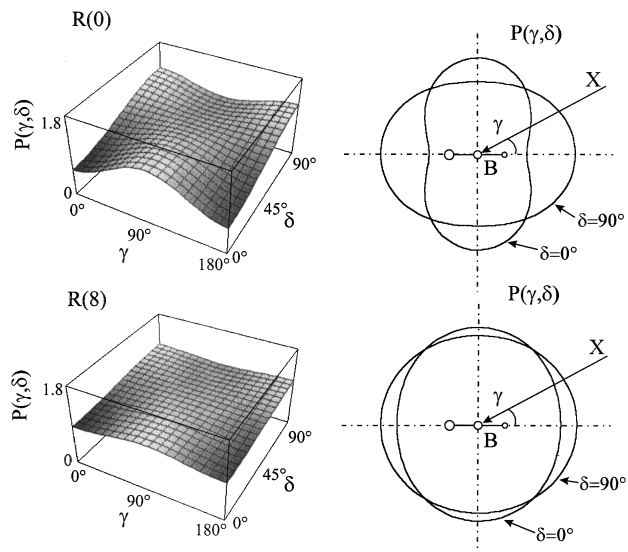
these two experimental situations $\vec{E}_v\|\vec{E}_J$ ($\delta=0°$) and $\vec{E}_v\perp\vec{E}_J$ ($\delta=90°$). An attack of the approaching atom A on one end of the B–C molecule, i.e. $\gamma=0$, is preferred for $\delta=0°$ ($\vec{E}_v\|\vec{E}_J$), in comparison to a perpendicular alignment of the two $\vec{E}$ vectors, i.e. $\delta=90°$. In contrast, a side-on reaction geometry, i.e. $\gamma=90°$, is preferred for $\delta=90°$ ($\vec{E}_v\perp\vec{E}_J$).

Qualitatively this situation is independent of which branch, P or R, and which rotation [with the exception of $P(1)$ excitation] is used to study the reaction dynamics. However, the differences in the reactivity for different polarization schemes are reduced in comparison to $R(0)$ excitation (Fig. 2).

Figure 4 shows $P(\gamma,\delta)$ for $\beta=-1$ (perpendicular transition), as is quite often observed in dissociation processes that may serve as sources for the A atom. In this case a linear approach of atom A on one end of the BC molecule ($\gamma=0$) is preferred for $\delta=90°$ ($\vec{E}_v\perp\vec{E}_J$), while a side-on approach is preferred for $\delta=0°$.

Due to intensity variation under different polarization schemes we can distinguish between a preferred linear or a preferred perpendicular reaction geometry. We would also like to gain some insight into how far the angle of attack deviates from $\gamma=0°$ for an exactly linear approach or from $\gamma=90°$ for an exactly perpendicular approach, respectively. In the following we will assume an essentially linear reaction geometry and the reaction probability should not change as long as the attack angle γ is within a cone of acceptance limited by γ_{max}. Outside of this cone no reaction takes place, i.e. the opacity function $f(\gamma)$ is constant for $0 \leqslant \gamma \leqslant \gamma_{max}$ and vanishes for $\gamma > \gamma_{max}$. The measured signal for a given polarization, i.e. a selected angle δ, is then obtained by integrating Eq. (7) from $\gamma=0°$ to $\gamma=\gamma_{max}$. Thus, the steric effect of the reaction, SE, is given by

$$SE(\gamma_{max}) = \frac{\int_0^{\gamma_{max}} P_J(\gamma, \delta = 90°)\sin(\gamma)\,d\gamma}{\int_0^{\gamma_{max}} P_J(\gamma, \delta = 0°)\sin(\gamma)\,d\gamma}. \tag{9}$$

The integration of this equation can easily be performed.[8]

It should be mentioned that depolarization effects due to the earth magnetic field and the nuclear spin of reactant B are not considered.[10–12] Precession of the nuclear spin leads to a decrease of the initial molecular alignment. The depolarization is stronger for low J values. For high rotations the total angular momentum F is essentially determined by J, because typical values of I, the nuclear spin, are below $\frac{5}{2}$. In the high J limit $A_0^{(2)}$ becomes independent of the excitation branch and Eq. (7) reduces to ($\delta = 0$),

$$P(\gamma, 0) \propto \left(1 + \frac{\beta}{10} P_2(\cos \gamma)\right). \tag{10}$$

The influence of the nuclear spin on the polarization measurements can also be neglected, if the time of precession τ_p is long compared to the observation (delay) time τ. On the other hand, if the interaction between J and I is strong, i.e. $\tau_p \ll \tau$, then a time-averaged depolarization coefficient can be calculated.[12]

The derivation of the above equations further assumes stationary target and precursor molecules. However, Gilbert et al.[13] have shown that the degradation in alignment is not likely to compromise seriously the viability of the experiment. Even if the reduction in alignment cannot be neglected completely in some cases (very heavy attacking atom and a very light target molecule), it can be adequately treated through an effective β parameter [Eq. (9) of Ref. 13].

III. COMPARISON WITH EXPERIMENTAL RESULTS

We have studied the reaction of aligned hydrogen atoms generated in the 266 nm photodissociation of methylmercaptan, CH_3SH, with HCN being excited (around 1.53 μm) in a single rotational state of the first overtone of ν_3 CH stretching motion. Details of the experimental setup are given elsewhere.[14,15] The β parameter for the $CH_3SH + h\nu \rightarrow H + CH_3S$ process is known to be $\beta \cong -0.96$[16,17] and, thus, a reaction plane is defined in the lab frame, as indicated by Fig. 1. The reaction H+HCN is endothermic and only rovibrationally excited molecules can react with the photolytically generated hydrogen atoms.[18,19] The collision energy and its distribution can be extracted from the experimental work of Wilson et al.[15] and is published elsewhere.[20] Chlorine atoms are generated in the photodissociation of Cl_2 at 355 nm and its spatial distribution is described by $\beta = -1$.[21] The CN product molecules were analyzed by LIF. The delay time between the CN analysis pulse and the HCN excitation laser pulse was 50 and 250 ns, depending on the system under investigation. Since the partial pressures were slightly below 10 Pa single collision conditions are expected and the product yield is directly proportional to the reactivity of the (aligned) reactants. The CN ($^2\Sigma \leftarrow X\ ^2\Sigma$) transition is saturated and, thus, any influence of aligned CN products on the signal can be neglected.

TABLE I. Observed steric effect, $(I_\perp - I_\parallel)/(I_\perp + I_\parallel)$, in the reaction of H+HCN(ν_3) with $\nu_3 = 2,4$ and Cl+HCN ($\nu_3 = 2$, $J = 9$). The error of the intensity ratio is below 0.01. The positive values indicate a linear reaction geometry for both the Cl and the H atom reaction.

Reaction	Transition	Delay time/ns	$(I_\perp - I_\parallel)/(I_\perp + I_\parallel)$
H+HCN ($\nu_3 = 2$, $J = 1$)	$R(0)$	50	0.065
H+HCN ($\nu_3 = 2$, $J = 6$)	$R(5)$	50	0.022
H+HCN ($\nu_3 = 2$, $J = 0$)	$P(1)$	50	0.00
H+HCN ($\nu_3 = 2$, $J = 5$)	$P(6)$	50	0.01
H+HCN ($\nu_3 = 4$, $J = 9$)	$R(8)$	230	0.043
Cl+HCN ($\nu_3 = 2$, $J = 9$)	$R(8)$	230	0.029

The measured intensity ratios $(I_\perp - I_\parallel)/(I_\perp + I_\parallel)$ for different reactions are summarized in Table I, where the subscripts $\parallel$ or $\perp$ indicate a parallel or perpendicular alignment between $\vec{E}_J$ and $\vec{E}_V$. The polarization of the lasers were rotated by using $\lambda/2$ wave plates[22] of zeroth order. The beam walk has not been observed. Four hundred laser shots for each polarization scheme were averaged to obtain the data. The data for $P(1)$ excitation were used to minimize systematic errors due to beam walk or lengthy data averaging. The observed deviation for $P(1)$ excitation was always below ± 0.01. The positive intensity ratio demonstrates a preferred end-on attack of the hydrogen or the chlorine atom on the hydrogen atom of the HCN molecule. Thus, a linear reaction geometry is preferred for both the H+HCN$\rightarrow$H$_2$+CN and the Cl+HCN$\rightarrow$HCl+CN reaction. The observed intensity ratios of the different transitions at a delay time of 50 ns behave as one expects when Eq. (2) is considered. However, HCN exhibits a nuclear spin and a quadrupole moment that will strongly depolarize the initial aligned HCN. Since this effect becomes negligible for high rotations [Eq. (10)] or for delay times $\leqslant 50$ ns, the range of the angle of attack, $[0, \gamma_{max}]$, can be extracted from Eq. (9).[22] We obtain $\gamma_{max}[H+HCN(\nu_3=2)]=50°$, $\gamma_{max}[H+HCN(\nu_3=4)]=55°$, and $\gamma_{max}[Cl+HCN(\nu_3=2)] = 65°$. Since the experimental error is ca. $\pm 5°$, we assume that the cone of acceptance is slightly larger for the Cl reaction in comparison to the H+HCN reaction.

In principle, there is the possibility of significant reagent reorientation on an approach to the transition state. However, all performed measurements with rovibrationally excited HCN as well as all trajectory studies indicate a similar behavior for both the H and the Cl reaction,[15,20] and a long living transition state can be excluded. Since the approach of the light and fast hydrogen atom is unlikely to reorientate the HCN, we assume no substantial reagent reorientation.

IV. SUMMARY

The reaction geometry can be analyzed even in bulk experiments when polarized light is used. Equations have been developed that allow a relatively easy conversion of experimental results to the angle of attack, γ. At high reactant rotations the dynamic range of the signal intensities at different polarization schemes is fairly low, but sufficient to obtain a quantitative impression of the attack angle. For low

rotational states a larger intensity ratio can be expected, provided the influence of depolarization effects can be reduced. This becomes possible when a sufficient short delay time between preparation of the reactant and probe of the product can be used.

ACKNOWLEDGMENT

APPENDIX

We write for ρ_J in a normalized form [i.e., without overall factors $j/3$ and $(j+1)/3$, resp.],

$$\rho_J(\theta,\phi) = \frac{1}{\sqrt{4\pi}}\left(Y_{00} + \frac{A_0^{(2)}}{\sqrt{5}}Y_{20}(\theta,\phi)\right) \qquad (A1)$$

with $A_0^{(2)}$ for the P and R branch as given above. For ρ_v we write in a similar manner,

$$\rho_v(\vartheta,\varphi) = \frac{1}{\sqrt{4\pi}}\left(Y_{00} + \frac{\beta}{\sqrt{5}}Y_{20}(\vartheta,\varphi)\right), \qquad (A2)$$

where (ϑ,φ) reminds us of the fact that the z axis (i.e., $\vartheta = 0$) is different from the z axis for $\rho_J(\theta = 0)$. In fact, both enclose the angle δ, which is the angle between the two laser polarization directions $\vec{E}_v$ and $\vec{E}_J$.

We want to calculate the probability for a certain angle γ between (θ,ϕ) of ρ_J and (θ',ϕ') of ρ_v, i.e., the integral

$$\int_\Omega \int_{\Omega'} [\rho_J(\theta,\phi)\rho_v(\theta',\phi')]_\gamma \, d\Omega' \, d\Omega, \qquad (A3)$$

where the primes mark different integration variables, and $[\ ]_\gamma$ indicates that we have to confine ourselves to a fixed angle γ between (θ,ϕ) and (θ',ϕ'). Thus, the integral is not a fourfold, but only a threefold one.

At first, we use the rotational properties of the spherical harmonics Y_{lm} to rotate $\rho_v(\vartheta,\varphi)$ by an angle of δ about the y axis, in order to have the same system of axis for both (θ,ϕ) and (θ',ϕ'). This leads us to

$$\rho_v(\vartheta,\varphi)$$
$$= \frac{1}{\sqrt{4\pi}}\left(Y_{00} + \frac{\beta\sqrt{4\pi}}{5}\sum_m Y_{2-m}(\delta,0)Y_{2m}(\theta',\phi')\right).$$
$$\qquad (A4)$$

The integral can now be calculated in the form

$$\int_\Omega \rho_J(\theta,\phi)\left(\int_0^{2\pi}\rho_v(\theta'(\tau),\phi'(\tau))\sin\gamma \, d\tau\right)d\Omega \qquad (A5)$$

where (θ',ϕ') run through a cone with opening angle γ. The axis of the cone points to the direction of the outer integration variables θ,ϕ. To transform θ' and ϕ' to variables referring to the direction of the outer variables θ and ϕ once more we have to rotate the axis of $\rho_v(\theta',\phi')$ so that its z' axis points to the direction θ,ϕ. This yields, for $\rho_v(\theta',\phi')$,

$$\rho_v(\theta',\phi') = \frac{1}{\sqrt{4\pi}}\left(Y_{00} + \frac{\beta\sqrt{4\pi}}{5}\sum_m Y_{2-m}(\delta,0)\right.$$
$$\left. \times \sum_{m'} R_{mm'}(\theta,\phi)Y_{2m'}(\theta'',\phi'')\right), \qquad (A6)$$

where $R_{mm'}$ denotes the rotation matrix elements for the Y_{2m} set and the integral now reads as

$$\int_\Omega \rho_J(\theta,\phi)\frac{1}{\sqrt{4\pi}}\int_0^{2\pi}\left(Y_{00} + \frac{\beta\sqrt{4\pi}}{5}\sum_m Y_{2-m}(\delta,0)\right.$$
$$\left. \times \sum_{m'} R_{mm'}(\theta,\phi)Y_{2m'}(\gamma,\tau)\right)\sin\gamma \, d\tau \, d\Omega, \qquad (A7)$$

where we have fixed θ'' to γ. ϕ'' becomes the third integration variable τ. The τ integration can easily be performed, because

$$\int_0^{2\pi} Y_{2m'}(\gamma,\tau)d\tau = \begin{cases} 2\pi Y_{20}(\gamma), & \text{for } m' = 0, \\ 0 & \text{for } m' \neq 0. \end{cases} \qquad (A8)$$

Thus, Eq. (A7) simplifies to

$$\sqrt{\pi}\cdot\sin\gamma\int_\Omega \rho_J(\theta,\phi)\left(Y_{00} + \frac{\beta}{5}\frac{4\pi}{\sqrt{5}}\right.$$
$$\left. \times \sum_m Y_{2-m}(\delta,0)Y_{2m}^*(\theta,\phi)Y_{20}(\gamma,0)\right)d\Omega, \qquad (A9)$$

when R_{m0} is replaced by $\sqrt{4\pi/5}Y_{2m}^*$.

The integrals

$$\int_\Omega \rho_J(\theta,\phi)Y_{1m}^*(\theta,\phi)d\Omega = c_l^m \quad (l = 0,2), \qquad (A10)$$

are the expansion coefficients of ρ_J into spherical harmonics, which are

$$c_0 = \frac{1}{4\pi} \quad \text{and} \quad c_2^0 = \frac{1}{\sqrt{4\pi}}\frac{1}{\sqrt{5}}A_0^{(2)}. \qquad (A11)$$

After replacing the spherical harmonics by the corresponding Legendre Polynomials, we obtain the final result:

$$P(\gamma,\delta) \propto \frac{\sin\gamma}{2}\left(1 + \frac{\beta}{5}A_0^{(2)}P_2(\cos\delta)P_2(\cos\gamma)\right). \qquad (A12)$$

After adding the overall factors $J/3$ for the P branch and $(J+1)/3$ for the R branch we obtain Eqs. (6a) and (6b).

[1] D. H. Parker, K. K. Chakravorty, and R. B. Bernstein, J. Phys. Chem. **85**, 466 (1981).

[2] M. J. J. Vrakking and S. Stolte, Chem. Phys. Lett. **271**, 209 (1997); J. Bulthuis, J. J. van Leuken, and S. Stolte, Chem. Soc. Faraday Trans. **91**, 205 (1995); J. W. G. Mastenbroek, C. A. Taatjes, K. Nauta, M. H. M. Janssen, and M. S. Stolte, J. Phys. Chem. **99**, 4360 (1995).

[3] J. J. van Leuken, J. Bulthuis, S. Stolte, and H. J. Loesch, J. Phys. Chem. **99**, 13582 (1995).

[4] H. J. Loesch and A. Remscheid, J. Chem. Phys. **93**, 4779 (1990).

[5] B. Friedrichs and D. R. Herschbach, Nature (London) **353**, 412 (1991).

[6] R. N. Zare and D. R. Herschbach, Proc. IEEE **51**, 173 (1963).

[7] R. N. Zare, Ber. Bunsenges Phys. Chem. **86**, 422 (1982).

[8] R. N. Zare, Angular Momentum, *Understanding Spatial Aspects in Chemistry and Physics* (Wiley Interscience, New York, 1988).

[9] W. R. Simpson, T. P. Rakitzis, S. A. Kandel, A. J. Orr-Ewing, and R. N. Zare, J. Chem. Phys. **103**, 7313 (1995).

[10] R. Altkorn and R. N. Zare, Mol. Phys. **55**, 1 (1985).

[11] C. H. Greene and R. N. Zare, Annu. Rev. Phys. Chem. **33**, 119 (1982).

[12] A. J. Orr-Ewing and R. N. Zare, Annu. Rev. Phys. Chem. **45**, 315 (1994).

[13] E. P. Gilbert, G. Maitland, A. Watson, and K. G. McKendrick, J. Chem. Soc. Faraday Trans. **89**, 1527 (1993).

[14] C. Kreher, Ph.D. thesis, Frankfurt, 1996.

[15] C. Kreher, R. Theinl, and K.-H. Gericke, J. Chem. Phys. **104**, 4481 (1996).

[16] E. Jensen, J. S. Keller, G. C. G. Waschewsky, J. E. Stevens, and R. L. Graham, J. Chem. Phys. **98**, 2882 (1993).

[17] S. H. S. Wilson, M. N. R. Ashfold, and R. N. Dixon, J. Chem. Phys. **101**, 7538 (1994).

[18] J. Berkowitz, G. B. Ellison, and G. Dutman, J. Phys. Chem. **98**, 2744 (1994).

[19] M. J. Frost, I. W. Smith, and R. D. Spencer-Smith, J. Chem. Soc. Faraday Trans. **89**, 2355 (1993).

[20] C. Kreher, J. L. Rinnenthal, and K.-H. Gericke, to be published.

[21] Y. Matsumi, K. Tonokura, M. Kawasaki, J. Chem. Phys. **97**, 1065 (1992).

[22] K.-H. Gericke, C. Kreher, and J. L. Rinnenthal, J. Phys. Chem. (to be published).